Solution of the Perturbation Equation in Optical Tomography Using Weight Functions as a Transform Basis

Erh-Ya Lin*, Yao Wang*, Yaling Pei*, and Randall L. Barbour#
* *Polytechnic University, Brooklyn, NY 11201 and* #SUNY Health Science Center, Brooklyn, NY 11203

Abstract

This paper describes a new inverse solver for optical tomography. As with prior studies, we employ an iterative perturbation approach, which at each iteration requires the solution of a forward problem and an inverse problem. The inverse problem involves the solution of a linear perturbation equation, which is often severely underdetermined. To overcome this problem, we propose to represent the unknown image of optical properties by a set of linearly independent basis functions, with the number of basis functions being equal to or less than the number of independent detector readings. The accuracy of the solution depends on the choice of the basis. We have explored the use of the weight functions associated with different source and detector pairs (i.e. the rows in the weight matrix of the perturbation equation) as the basis functions. By choosing those source and detector pairs which have uncorrelated weight functions, the inverse problem is transformed into a well-posed, uniquely determined problem. The system matrix in the transformed representation has a dimension significantly smaller than the original matrix, so that it is feasible to perform the inversion using singular value decomposition (SVD). This new method has been integrated with a previously reported forward solver, and applied to data generated from numerical simulations using diffusion approximation. Compared to the Conjugate Gradient Descent (CGD) method used in previously reported studies, the new method takes substantially less computation time, while providing equal, if not better, image reconstruction quality at similar noise levels.

Keywords (100.3010) Image reconstruction techniques; (100.3080) Infra-red imaging.

Introduction

The imaging problem in optical tomography deals with the reconstruction of the absorption and the scattering coefficients of a heterogeneous scattering medium from the measurements of multiple scattered light signals on the medium surface. The problem is inherently difficult because the scattered field is non-linearly related to the optical properties of the underlying medium. To overcome this difficulty, we have developed an iterative perturbation approach [1,2]. Each iteration involves the solution of a forward problem to set up a new perturbation equation, and the solution of the perturbation equation, which constitutes the inverse problem. This approach is equivalent to the Gauss-Newton method (also known as Newton method). When Tikhonov regularization is employed in the least squares solution, it leads to the Levenberg-Marquardt method. The same overall approach has been taken by research groups of Arridge [3] and Paulsen [4,5], although our approaches to solving the forward and inverse problems differ from theirs.

One challenging problem in solving the perturbation equation,

$$\mathbf{Wx}=\mathbf{y}, \tag{1}$$

is that the affordable number of source and detector (SD) pairs, M, is usually substantially smaller than the number of unknowns, N. That is, the system is *severely underdetermined*. Among many possible solutions, we are interested in obtaining the *minimum norm solution*, which is equivalent to finding the minimal perturbation from the previous reconstruction to satisfy the measurement data. Theoretically, one can obtain this solution using singular value decomposition (SVD) of the weight matrix $\mathbf{W}$ [6]. However, the very large dimension of $\mathbf{W}$ can make the computation of SVD unfeasible in terms of both computation time and memory requirement. To overcome this problem, we have adopted the Conjugate Gradient Descent (CGD) method in our prior studies [1], which obtains the solution by minimizing the error norm $\|\mathbf{Wx}-\mathbf{y}\|^2$ through a conjugate gradient descent scheme. A problem with this approach is that the resulting solution depends on the initial solution. There is no easy way to guarantee the solution is minimum norm. In our previous studies, the initial solution is set to zero, which usually gives good solutions.

Paulsen, *et al.* uses Gauss elimination to solve the normal equation associated with the perturbation equation. The problem with this approach is that it gives a meaningful (least squares) solution only when the system is overdetermined. When the problem is severely underdetermined, the solution can be far from the desirable one. For this reason, in their earlier work, a coarse mesh is used to represent the target medium so that the number of

OSA TOPS Vol. 21 Advances in Optical Imaging and Photon Migration, James G. Fujimoto and Michael S. Patterson (eds.)

elements is roughly the same as the number of SD pairs. However, using a coarse mesh hinders the accuracy of the forward solver, and consequently the accuracy of the reconstructed image. Sufficiently accurate results can be obtained only when the object size is large relative to the medium size [4]. In order to overcome the underdetermined problem, they proposed a dual mesh technique that uses a fine mesh for the forward solution, but a coarse mesh for the inverse solution. Very good reconstruction results have been obtained from experimental data for a test medium containing a single target [5].

In this paper, we propose a new method for solving the perturbation equation which is significantly faster than the CGD method and the direct SVD method, when the number of SD pairs is an order of magnitude smaller than the number of unknowns.

The WTSVD Method

As described in Introduction, the perturbation equation given in Eq. (1) is usually severely underdetermined. In addition, depending on the SD configurations, many rows in the weight matrix (the weight functions) may not be linearly independent, which causes the weight matrix to be rank deficient. Rather than solving this ill-posed linear equation directly, we first perform a preprocessing on the original perturbation equation to delete rows that are known to be correlated *a priori*, we then apply a linear transformation to the unknowns before using SVD to solve the transformed equation.

Preprocessing of the Perturbation Equation

In general, with an arbitrary SD configuration, one needs to apply some sophisticated operation to derive independent rows in the weight matrix. However, in the most common SD configuration, in which the sources and detectors share the same set of locations, there is a simpler way. Because of the symmetry of $\mathbf{r}_s$ and $\mathbf{r}_d$ in the integral formula for calculating the weight matrix, exchanging source and detector positions gives us the same weight functions, and therefore the rows in the weight matrix that corresponding to these two pairs of SD are correlated. Instead of solving the original equation, we replace every two rows in the augmented matrix **[W y]** that correspond to the two SD pairs with exchanged positions by their average. The SD pairs that do not have counterparts are those where the source and detectors are co-located. Because the detector readings at exactly the source locations are not very informative, we choose not to use these SD pairs. It is easy to show that the number of rows after such a reduction is $K=L(L-1)/2$, where L represents the number of SD locations. To make the solution of the equation more stable numerically, we further normalize the row vectors in the resulting weight matrix. We denote the resulting equation as

$$\tilde{\mathbf{W}}\mathbf{x}=\tilde{\mathbf{y}} \qquad (2)$$

Transformed Representation Using Weight Functions

With the transformed representation, the unknown **x** is spanned by the row vectors $\tilde{\mathbf{w}}_k$ in the weight matrix as

$$\mathbf{x}=\sum_k t_k \tilde{\mathbf{w}}_k = \tilde{\mathbf{W}}^T\mathbf{t} \qquad (3)$$

where $\mathbf{t}=[t_1, t_2, \ldots, t_K]^T$. Substituting Eq. (3) into Eq. (2) leads to

$$\mathbf{At}=\tilde{\mathbf{y}} \quad \text{with} \quad \mathbf{A}=\tilde{\mathbf{W}}\tilde{\mathbf{W}}^T. \qquad (4)$$

Once **t** is determined by solving the above transformed equation, one can derive the desired solution by using Eq. (3), which can be considered as the inverse transform. The overall solution can be represented as

$$\mathbf{x}=\tilde{\mathbf{W}}^T(\tilde{\mathbf{W}}\tilde{\mathbf{W}}^T)^{-1}\tilde{\mathbf{y}}. \qquad (5)$$

With the weight functions as the basis functions, as given in Eq. (3), the contribution of each SD pair to the final solution is in the form of the weight function associated with it. *Since the weight functions tell us where we can see the object more clearly given a source and detector pair, by using this transformation basis, we only try to solve the part of the object that can be seen by the source and detector pairs used, thus reducing the ambiguity of the inverse problem.* The reconstruction of the original unknowns **x** from the transformed vector **t**, i.e., the inverse transform in Eq. (3), resembles the well known back-projection process. It is easy to recognize that the final solution in Eq. (5) is in fact the minimum-norm solution for an underdetermined system with rank equal to the number of rows. Note that the *ij*-th element in the transformed matrix **A** is $a_{ij}=(\tilde{\mathbf{w}}_i,\tilde{\mathbf{w}}_j)$, the inner product of the normalized weight functions of two SD pairs. This ensures that the diagonal elements in **A** is equal to or larger than the off-diagonal elements. Although we still need to solve a linear equation, the properties of $\mathbf{A}$ are very different from that of $\tilde{\mathbf{W}}$. A is a square symmetric matrix with a dimension equal to the number of uncorrelated SD pairs, and it is diagonally dominant in that all diagonal elements are one and off-diagonal terms are less than one in magnitude. The decay of the off-diagonal elements, however, is not very rapid.

Solution of the Transformed Equation

Theoretically, as long as the K normalized weight functions are independent, then the square matrix **A** is guaranteed to be non-singular, and the transformed equation (4) can be solved reliably using the simplest inversion method --- the Gauss elimination method. In practice, however, some rows in the weight matrix could still be correlated, and the Gauss elimination method may lead to unstable solutions. In order to circumvent this problem, we solve the transformed equation using the SVD method with Tikhonov regularization. This is feasible because the dimension of **A**, K, is usually on the order of hundreds, for a practically feasible number of SD pairs. For example, if $L=18$, than

K=153. The incorporation of regularization is to suppress the noise effect. Let α_k represent the singular value of **A**, arranged in a descending order, and $\mathbf{u}_k$ and $\mathbf{v}_k$ the corresponding left and right singular vectors, the regularized SVD solution of Eq. (4) is

$$\mathbf{t}=\sum_k \left(\frac{\alpha_k}{\alpha_k^2+\lambda^2}\right)(\mathbf{u}_k,\tilde{\mathbf{y}})\,\mathbf{v}_k \quad . \tag{6}$$

The regularization parameter λ is chosen based on the Miller's L-curve criterion [7].

Simulation Results

The proposed method has been used to accomplish simultaneous reconstruction of absorption and diffusion coefficients from numerically calculated data for several test media. In all the simulations, a frequency modulated source is employed with a modulation frequency of 200 MHz. The detector measures the photon density on the surface, which is a complex variable. All the test media have a circular boundary with a radius of 4 cm. The medium is represented with an FEM mesh with 1800 nodes so that the number of unknowns is *N*=3600 (2 unknowns for each node). This spatial resolution is used for both the forward and inverse calculations. The sources and detectors are located uniformly on the circular boundary sharing the same set of locations. Two SD configurations are tested, with 10x10 (*L=10,K=45*) and 18x18 (*L=18,K=153*) SD pairs, respectively. The forward calculation is based on the diffusion approximation using an FEM method, using the Dirchlet boundary condition [8]. For the inverse problem, we compared the WTSVD method and the CGD method. With the CGD method, the original perturbation equation is solved directly. The number of iterations at each perturbation step varies but is limited to at most 1000 iterations. With both methods, the perturbation iteration stops when the ratio of the energy (sum of squares) of the current perturbation solution to the energy of the total perturbation until this iteration is less than 10^{-3}, or when the number of perturbations reaches 10. In the following, we describe the reconstruction results for two test media. The properties of these test media are summarized in Table 1. In either case, the initial estimate is set to the same as the background medium.

Test Medium I Figure 1 shows the reconstructed images under different test conditions. In the noise free case, the results obtained using WTSVD and CGD are very similar when 10x10 SD pairs are used, with the reconstructed objects having a size noticeably larger than the true object size. With 18x18 SD pairs, the shape of the reconstructed object by the WTSVD method is very close to the true object, better than the CGD result. In the noise-added case (10% or 20dB), the reconstructed object by WTSVD is blurred compared to the noise-free case, but the object structure is clearly visible. The CGD method has produced a similar reconstruction result. Figure 2 plots the root mean square error (RMSE) between the reconstructed $\Delta\mu_a$ and ΔD and the true $\Delta\mu_a$ and ΔD. This plot clearly shows that the WTSVD method converges faster than the CGD method.

Test Medium II Figure 3 shows reconstruction results under different test conditions, all obtained with 18x18 SD pairs. The reconstructed ΔD images have a severe ringing artifact initially, which gradually goes away with more iterations. It can be seen that images obtained with WTSVD is much sharper than with CGD. With both WTSVD and CGD method, the true $\Delta\mu_a$ values are underestimated, whereas the recovered ΔD values are quantitatively accurate. With noise-added data (3% or 30 dB), the object is blurred, but is reconstructed at the right location. At higher noise levels, reconstructed images after first one or two iteration usually were correct in terms of location and contrast of the objects, but the reconstruction results after subsequent iterations become unacceptable. We have found that the reconstruction of a medium with two objects is more sensitive to noise than a medium with a single object. Also, reconstruction from 18x18 SD set-up is more sensitive to noise than from 10x10 SD set-up. Figure 4 compares the RMSEs of the reconstructed $\Delta\mu_a$ and ΔD after different iterations, using the WTSVD and CGD methods, respectively. In this case, the WTSVD method yielded lower RMSE for both $\Delta\mu_a$ and ΔD after one iteration, than CGD. But upon convergence, the WTSVD has a higher RMSE for $\Delta\mu_a$, but lower RMSE for ΔD. Note that with the CGD method, the RMSE for $\Delta\mu_a$ continues to decrease and eventually may become lower than that of WTSVD, but the RMSE for ΔD either stays flat or even increase with more iterations. Visually, the reconstructed ΔD image by the CGD method tends to become noisier on the boundary as the number of perturbations increases. The rational behind this also needs further investigation.

Comparison of Computational Complexity The results presented before showed that the WTSVD method and the CGD method achieves about the same quality, with the WTSVD method giving slightly sharper images with fewer boundary artifacts. The more noteworthy advantage of the WTSVD method is its reduced computation time. In our study, all the computations were done using a SUN Ultra SPARCstation with 290 Mbytes of memory. The forward part was implemented using Fortran. The CGD method was integrated with the forward code in a single Fortran code, while the WTSVD method was implemented using Matlab 4.2 platform. Table 2 summarizes the required computation time for different parts of the reconstruction algorithm for 10x10 and 18x18 SD cases. It is clear that the WTSVD method requires significantly shorter time in each iteration. For example, with 18x18 SD pairs, the computation time for each iteration (including both forward and inverse solutions)

is 13 minute with the WTSVD, while the CGD method requires 60 minutes. As described previously, the WTSVD method takes a smaller number of iterations to converge than the CGD method in the simulation results. Roughly, five iterations are sufficient with the WTSVD method, whereas ten or more iterations are needed for the CGD method. From Table 2, in the 18x18 SD case, 5 iterations using WTSVD will take 65 minutes, whereas 10 iterations using CGD would take 600 minutes, a saving factor of 10. Note that the computation time required by the WTSVD method is likely to be reduced further once it is implemented outside the Matlab environment.

Discussion

The proposed WTSVD algorithm has been shown to require significantly shorter computation time than the previously reported CGD method, while providing similar reconstruction quality. It not only requires less time to solve the perturbation equation in each iteration, but also requires fewer iterations. The total saving factor is on the order of 10. Note that the computational advantage of the WTSVD method decreases when the number of SD pairs increases. Specifically, using an analysis of the flops required by different methods, we have found that the CGD algorithm will become more efficient, when the number of SD pairs exceeds 68x68.

The WTSVD method represents the unknown image using a basis consisting of normalized, independent weight functions. There may be other bases which can represent the unknown image better. Although using the weight functions enables one to attempt to recover the part of the image that can be "seen" by the SD pairs, they are not good basis functions in terms of their spatial-frequency support regions. Fourier or Wavelet basis functions may be more efficient in that with the same number of basis functions, these bases may represent an image more accurately. As a future research, we plan to investigate how to adapt standard wavelet bases to fit with node distributions in the finite element mesh representation of an arbitrarily shaped medium and explore the potential of using such bases for representing the unknown image.

The focus of this work is to examine the effectiveness of the WTSVD algorithm in solving a given perturbation equation and how does it compare with the CGD method in terms of accuracy, robustness, and computational complexity. Therefore, we have only tested for a fixed type of source and detector configuration and for the case when the initial estimate is the same as the background medium. When all such conditions are equal, we have indeed show that the WTSVD method can provide significant computation savings over the CGD method. It is not our intention to examine the capability of the overall perturbation approach in terms of minimally detectable target contrast and size, and the influence of the SD configurations on the reconstruction performance. Nor did we try to investigate the effect of the mismatch between the actual background medium and the assumed one on the convergence behavior of the overall reconstruction scheme. These issues will depend not only on the inverse algorithm, but also the forward algorithm. A thorough evaluation in this direction requires further investigation.

Acknowledgments

This work is supported in part by the NIH under grant 1-RO1-CA66184-01A2.

References

1. R. L. Barbour, H. L. Graber, Y. Wang, J.-H. Chang, and R. Aronson, "A Perturbation Approach for Optical Diffusion Tomography Using Continuous--Wave and Time--Resolved Data," In *Medical Optical Tomography --- Functional Imaging and Monitoring*, G. Muller ed., SPIE Inst. IS11, pp. 87--120, 1993.
2. Y. Yao, Y. Pei, Y. Wang, and R. L. Barbour, "A Born Type Iterative Method for Imaging of Heterogeneous Scattering Media and Its Application to Simulated Breast Tissue," in *Optical Tomography and Spectroscopy of Tissue: Theory, Instrumentation, Model, and Human Studies II*, Proc. SPIE, Vol. 2979, pp. 232-240, Feb. 1997.
3. S. R. Arridge, "The forward and inverse problems in time resolved infra-red imaging", In *Medical Optical Tomography --- Functional Imaging and Monitoring*, G. Muller ed., SPIE Inst. IS11, pp. 35-64, 1993.
4. H. Jiang, K. D. Paulsen, and U. L. Osterberg, "Optical image reconstruction using frequency-domain data: simulations and experiments," *J. Opt Soc. Am. A*, 13(2):253-266 (1996).
5. H. Jiang, K. D. Paulsen, U. L. Osterberg, and M. Patterson, "Frequency-domain optical image reconstruction in turbid media: an experimental study of single target detectability," *Applied Optics*, 36(1): 52-63 (1997).
6. H. Golub and C.F. Van Loan, *Matrix Computations*, Johns Hopkins Univ. Press. 2nd ed.,1991.
7. K. Miller, "Least squares methods for ill-posed problems with a prescribed bound," *SIAM J. Math. Anal.* 1: 52-74, (1970)
8. Y. Pei, Y. Yao, F.-B. Lin, and R. L. Barbour, "Frequency domain fluorescence optical imaging using a finite element method," in *Optical Tomography and Spectroscopy of Tissue: Theory, Instrumentation, Model, and Human Studies II*, Proc. SPIE, Vol. 2979, pp. 164-175, Feb. 1997.

Table 1 Optical Properties of Test Media

Test Cases	Background media			Target geometry		Target 1		Target 2	
	Radius	ua(cm^{-1})	us(cm^{-1})	Radius	Separation	ua(cm^{-1})	us(cm^{-1})	ua(cm^{-1})	us(cm^{-1})
Case I	4 cm	0.02	5	0.75 cm		0.04	10	N/A	N/A
Case II	4 cm	0.05	10	0.35 cm	1.5 cm	0.1	20	0.1	20

Table 2 Computer Time (in minutes) Required by Different Methods

Methods	One Iter.			5 Iter.	10 Iter.
	Forw.	Inv.	Total		
CGD10 (1000 iterations)	2.0	20.0	22	110	220
WTSVD10	2.5	1.5	4	20	40
CGD18 (1000 iterations)	6.0	54.0	60	300	600
WTSVD18	6.5	6.5	13	65	130

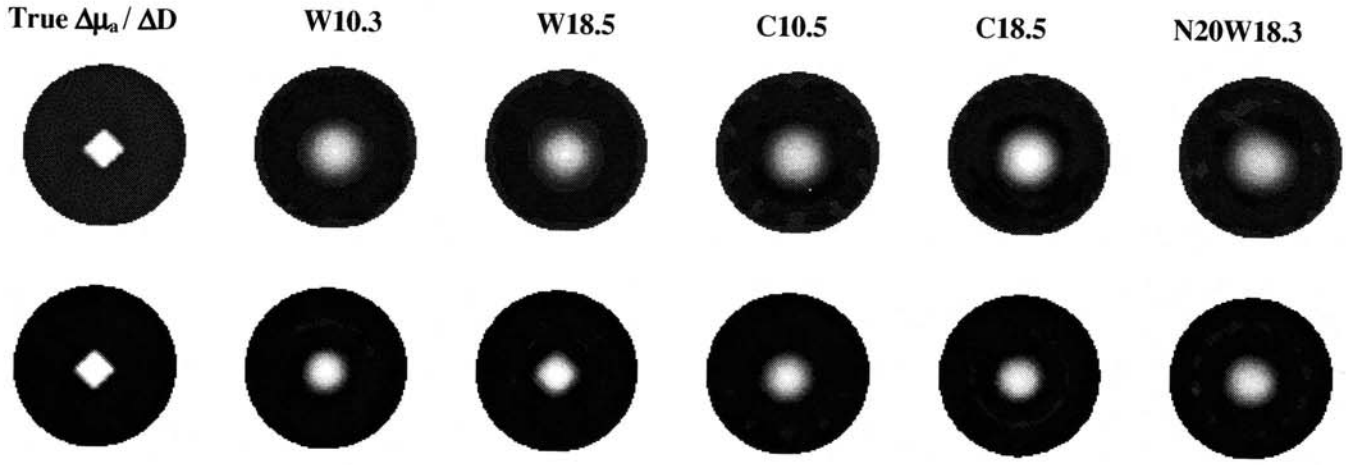

Figure 1 Reconstruction results for Test Medium I. Top row is for $\Delta\mu_a$ and bottom row for ΔD. From left to right are: 1) the true image; 2) and 3) reconstructed using WTSVD from noise-free data of 10x10 and 18x18 SD pairs, respectively; 4) and 5) reconstructed using CGD from noise-free data of 10x10 and 18x18 SD pairs, respectively; 6) reconstructed using WTSVD from noise-added data of 18x18 SD pairs, noise level is 10% (SNR=20dB). The last number in the label of each image indicates the number of iterations used.

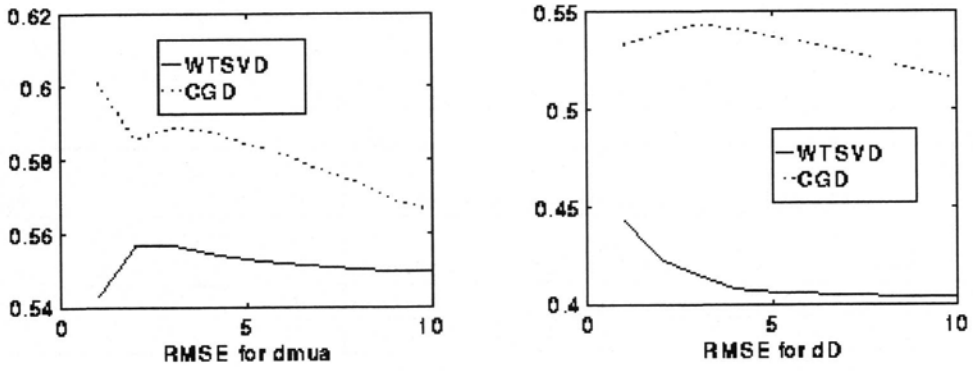

Figure 2 RMSEs of reconstructed images after successive iterations for Test Medium I.

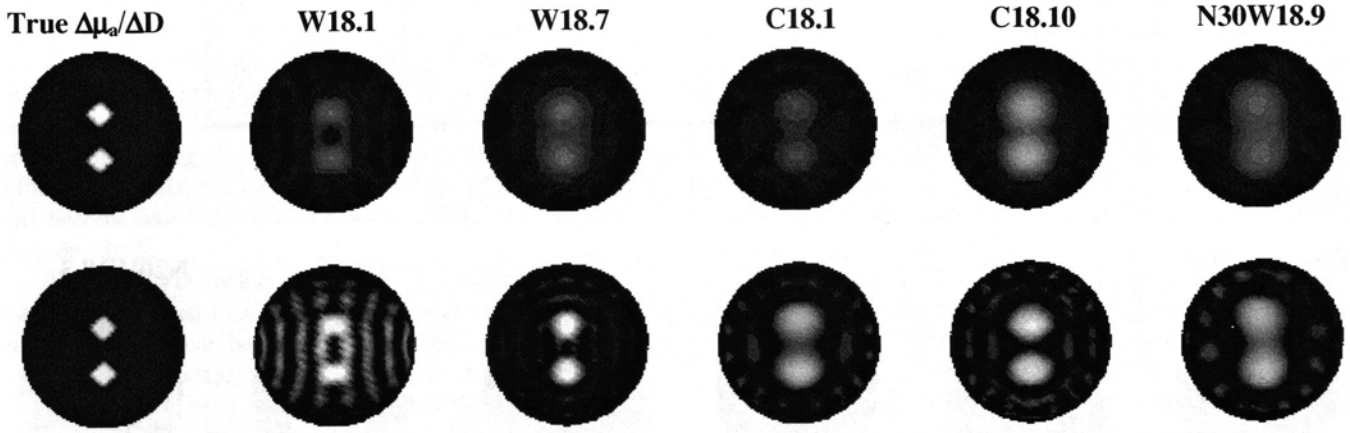

Figure 3 Reconstruction results for Test Medium II. Top row is for $\Delta\mu_a$ and bottom row for ΔD. From left to right are: 1) the true image; 2) and 3) reconstructed using WTSVD from noise-free data of 18x18 SD pairs, after 1 and 7 (reaching convergence) iterations, respectively; 4) and 5) reconstructed using CGD from noise-free data of 18x18 SD pairs, after 1 and 10 iterations respectively; 6) reconstructed using WTSVD from noise-added data of 18x18 SD pairs, noise level is 3% (SNR=30dB).

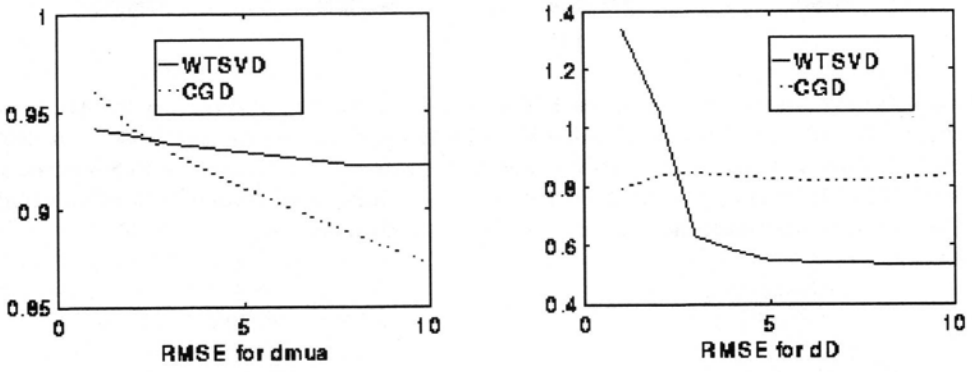

Figure 4 RMSEs of reconstructed images after successive iterations for Test Medium II.